

# Formulations of Artificial Viscosity for Multi-dimensional Shock Wave Computations

E. J. Caramana, M. J. Shashkov, and P. P. Whalen

*Hydrodynamics Methods Group, Mathematical Modelling and Analysis Group, Applied Theoretical  
and Computational Physics Division, Theoretical Division, Los Alamos National Laboratory,  
P.O. Box 1663, MS D413, Los Alamos, New Mexico 87545*

Received June 16, 1997; revised March 13, 1998

---

In this paper we present a new formulation of the artificial viscosity concept. Physical arguments for the origins of this term are given and a set of criteria that any proper functional form of the artificial viscosity should satisfy is enumerated. The first important property is that by definition a viscosity must always be dissipative, transferring kinetic energy into internal energy, and must never act as a false pressure. The artificial viscous force should be Galilean invariant and vary continuously as a function of the criterion used to determine compression and expansion, and remain zero for the latter case. These requirements significantly constrain the functional form that the artificial viscous force can have. In addition, an artificial viscosity should be able to distinguish between shock-wave and adiabatic compression, and not result in spurious entropy production when only the latter is present. It must therefore turn off completely for self-similar motion, where only a uniform stretching and/or a rigid rotation occurs. An additional important, but more subtle, condition where the artificial viscosity should produce no effect is along the direction tangential to a convergent shock front, since the velocity is only discontinuous in the normal direction. Our principal result is the development of a new formulation of an edge-centered artificial viscosity that is to be used in conjunction with a staggered spatial placement of variables that meets all of these standards, and without the need for problem dependent numerical coefficients that have in the past made the artificial viscosity method appear somewhat arbitrary. Our formulation and numerical results are given with respect to two spatial dimensions but all of our arguments carry over directly to three dimensions. A central feature of our development is the implementation of simple advection limiters in a straightforward manner in more than one dimension to turn off the artificial viscosity for the above mentioned conditions, and to substantially reduce its effect when strong velocity gradients are absent. © 1998 Academic Press

---

## 1. INTRODUCTION

The addition of a fictitious term, the artificial viscosity, into the inviscid Euler equations of fluid dynamics in order to automatically “capture” shock wave discontinuities in a fluid is perhaps the oldest numerical device in the relatively new field of computational physics and mechanics [1]. However, in the nearly half century since this idea was introduced it remains just a convenient and somewhat ad hoc numerical technique. Many different functional forms for the artificial viscosity have been proposed. These contain problem sensitive parameters that are often set in a somewhat arbitrary manner.

The purpose of this work is to remove as many of these arbitrary parameters and choices as possible and to define and delineate the issues critical to a successful form of artificial viscosity. We are interested in staggered spatial grid formulations in more than one dimension; in these schemes position and velocity are defined at the grid points or nodes, and all other variables, such as density and internal energy, are defined inside the zones whose boundaries are given by straight lines connecting the points. The new artificial viscosity presented in this paper is meant to be used with this kind of spatial differencing. However, a set of criteria that should be satisfied by any artificial viscosity is enumerated. These criteria provide relevant standards for evaluating these formulations.

The most basic property that an artificial viscosity must satisfy is dissipativity. That is, this term must always convert kinetic energy into internal energy and never the other way around. In more than one dimension this is a nontrivial requirement. This is herein addressed in terms of the new framework of “compatible formulations” of discrete systems of equations [2]. After this a number of additional properties that any successful artificial viscosity should have are considered. First, it must vanish for uniform compression and rigid rotation. It should also vanish along a surface of constant phase. Along such a surface the velocity field has a constant magnitude, and is also continuous, but may vary in direction. The direction that is tangential to the direction of propagation of a shock front is an example of this situation. This important property has been missed by many authors, but not by Schulz [3], and is of paramount importance for the accurate treatment of convergent flow problems. Finally, a useful artificial viscosity should produce forces that go to zero continuously as compression goes to zero and remain zero for expansion, so that the latter is a reversible process. Proper definitions of compression and expansion must be given in the multi-dimensional context. This is the task that this paper addresses. In pursuing it we will draw on a long history of past work and generalize some new ideas to more than one dimension.

This paper is organized as follows: In Section 2 the fundamental ideas and principles underlying the artificial viscosity method are introduced. This is done along the lines of previous work by requiring that the shock conditions be satisfied, and using an analogy with the completely inelastic collision of particle masses. After this the problem of a proper one-dimensional artificial viscosity is explored. The difficulty in constructing an artificial viscosity that vanishes for uniform compression is discussed, and the two different solutions to this problem that have been utilized are presented: One is the use of a tensor form that resembles the physical viscosity of a fluid; the other is the limiter formulation of Christiansen [4, 5]. Section 4 presents the main focus of our work. The concepts of an edge versus a zone centered artificial viscosity are introduced along with the differencing scheme that is employed to compute both the viscous forces and the work done by them. We present a general set of conditions that any functional form of the artificial viscosity should satisfy; the manner in which dissipativity is ensured is explained. The generalization of simple

advection limiters to a multi-dimensional framework for use with an artificial viscosity is given. It is shown how these act to turn off the artificial viscosity when physically necessary. Next, an edge-centered viscosity is formulated and analyzed with respect to our stated criteria and contrasted to the previous work of Schulz [3]. Finally, zone-centered artificial viscosities are briefly considered; it is shown that some misconceptions have arisen with regard to this form. Numerical results are presented in Section 5 that are meant to show the dependencies of our artificial viscosity on the parameter constants and on the limiters for both convergent and divergent shock wave problems. Other difficulties with the use of an artificial viscosity are detailed, and our conclusions are discussed. Last, an appendix is included that summarizes our recommended form of artificial viscosity in a succinct manner that is easy to code.

## 2. FUNDAMENTALS

The original formulation of the artificial viscosity introduced by VonNeumann and Richtmyer [1] involved adding a term to the momentum equation that essentially augments the scalar pressure in the instance where there is shock compression. This term was postulated, but constrained, by the requirements that solutions to the new system containing it satisfy the shock jump conditions and have a negligible effect outside the shock layer. The shock width so obtained is always the order of the finest grid spacing and has no physical scale, a fact that leads to the inherent difficulties and limitations associated with this method.

Consider a staggered grid in one-dimension where the density, pressure, and specific internal energy are defined in zones delineated by grid points where the coordinate position and velocity are specified. If  $\rho$  is the density of a zone across which the velocity has a difference  $\Delta\mathbf{v}$ , then this term, denoted as  $q_{nl}$ , is given by the nonlinear expression

$$q_{nl} = c_2 \rho (\Delta\mathbf{v})^2, \quad (1)$$

where  $c_2$  is a constant of order unity. Now the zone pressure,  $p_z$ , is augmented everywhere in the Euler equations by  $q_{nl}$ . These together act to prevent zone collapse in a time step  $\Delta t$  that is determined by the usual CFL stability condition  $c_s^* \Delta t / \Delta x \leq 1$ , where  $\Delta x$  is the zone width and  $c_s^*$  is a generalized sound speed in the zone based on the effective zone pressure  $p_z + q_{nl}$ . The term  $q_{nl}$  is dissipative if we require that it be nonzero only for zone compression; it then only converts kinetic energy, defined at the points or nodes, into zone internal energy. It thus acts as a viscosity.

The origin of Eq. (1) can be seen simply by considering the completely inelastic collision of two masses  $M_1$  and  $M_2$ . Then, although momentum is conserved, the decrease in the kinetic energy after the collision is  $\mu(\Delta\mathbf{v})^2/2$ , where  $\mu$  is the reduced mass and  $\Delta\mathbf{v}$  is the difference in the velocities of the two masses before the collision occurred. Thus, the functional form of the nonlinear artificial viscosity is that of the specific kinetic energy available for transfer to internal energy in a completely inelastic collision of two masses, where the density plays the role of the reduced mass. It is for this reason that the nonlinear artificial viscosity of Eq. (1) results in the same amount of zone compression independent of shock strength. If automatically contains the correct amount of kinetic energy to be dissipated. Although other forms of artificial viscosity that depend on  $\Delta\mathbf{v}$  to some power and have the dimensions of a pressure can be constructed, only the one given by Eq. (1) has this important property.

While the above form was found adequate to capture strong shocks, and does prevent zone inversion, unphysical oscillations were observed to occur behind the shock front. In order to eliminate these Landshoff [6] proposed that an additional term that vanishes less rapidly than Eq. (1) as one moves into the shocked material be added to the nonlinear term. This is given by

$$q_{lin} = c_1 \rho c_s |\Delta \mathbf{v}|, \quad (2)$$

where  $c_s$  is the usual zone sound speed based only on the zone pressure and  $c_1$  is a constant. This viscosity term was often found to produce too much spreading of the physical solution about a shock front. For this reason, and until very recently, the factor  $c_1$  was usually set an order of magnitude smaller than  $c_2$ .

We now have what will be referred to as the generic form of artificial viscosity. This is simply given by the addition of the linear and nonlinear terms as

$$q_{gen} = c_1 \rho c_s |\Delta \mathbf{v}| + c_2 \rho (\Delta \mathbf{v})^2. \quad (3)$$

Many formulations of artificial viscosity in more than one dimension use the form given by Eq. (3) with minor modifications. Usually these entail endowing it with directional properties of some sort and/or redefining  $\Delta \mathbf{v}$  as the product  $l_z \nabla \cdot \mathbf{v}^*$ , where  $l_z$  is some effective length through a zone or distance along the edge of a zone, and  $\nabla \cdot \mathbf{v}^*$  is the divergence of the velocity field with respect to some specified direction [7]. In one dimension and in slab geometry this reduces to  $\Delta \mathbf{v}$  and the form given by Eq. (3).

Our previous analogy of an artificial viscosity modelled on the inelastic collision between discrete particle masses that have a finite size can be carried further. Loosely following the work of Favorskii *et al.* [8, 9], consider an inelastic collision between a piece of mass  $\delta M_1$  that is a part of a mass  $M_1$ , with a piece of mass  $\delta M_2$  that is part of a mass  $M_2$ . Let these masses be infinitesimal in size and assume that they form a virtual particle of mass  $(\delta M_1 + \delta M_2)$ . Then if the velocities of the masses before this collision are  $\mathbf{v}_1$  and  $\mathbf{v}_2$ , we have from conservation of momentum that the velocity of the virtual particle  $\mathbf{v}^*$  is given by

$$(\delta M_1 + \delta M_2) \mathbf{v}^* = \delta M_1 \mathbf{v}_1 + \delta M_2 \mathbf{v}_2. \quad (4)$$

Now suppose that this virtual particle instantaneously splits apart with its respective mass components  $\delta M_1$  and  $\delta M_2$ , now with common velocity  $\mathbf{v}^*$ , recolliding with their original parent masses  $M_1 - \delta M_1$  and  $M_2 - \delta M_2$ , each with their unchanged initial velocities. The net result of this two step process is that mass  $M_1$  undergoes a change of momentum given by

$$M_1 (\mathbf{v}_{1f} - \mathbf{v}_1) = \frac{\delta M_1 \delta M_2}{(\delta M_1 + \delta M_2)} (\mathbf{v}_2 - \mathbf{v}_1), \quad (5)$$

where  $\mathbf{v}_{1f}$  is the final velocity of  $M_1$ . An analogous equation holds for  $M_2$  where the momentum transfer has the same magnitude as that given by Eq. (5) but, of course, with opposite sign. Now if we assume that  $\delta M_1 = \delta M_2 = \rho \mathcal{V} \tau$ , where  $\mathcal{V}$  is a generalized interaction velocity whose explicit form may vary somewhat and  $\tau$  is an interaction time, then the RHS of Eq. (5) becomes  $\rho \mathcal{V} (\mathbf{v}_2 - \mathbf{v}_1) \tau / 2$ . If we next specify that  $\mathcal{V} = |\mathbf{v}_1 - \mathbf{v}_2|$  and that the time  $\tau$  has the differential size  $dt$ , then the RHS of Eq. (5) becomes  $-\rho (\Delta v)_{12}^2 dt / 2$ , from which the familiar form of the effective nonlinear viscous pressure  $\rho (\Delta v)^2$  is apparent.

(Here we have assumed that  $\mathcal{V}$  or  $|\mathbf{v}_1 - \mathbf{v}_2|$  sweeps out a unit area.) In the one-dimensional case where the mass  $M_2$  lies to the right of  $M_1$ , and where there is in addition a mass  $M_0$  that lies to the left of  $M_1$  with velocity  $v_0$ , then Eq. (5) also contains a term associated with the interaction of  $M_1$  with mass  $M_0$ . Thus in the one-dimensional case the form of Eq. (5) becomes

$$M_1 \frac{dv_1}{dt} = [-\rho(v_1 - v_2)^2 + \rho(v_0 - v_1)^2]/2. \quad (6)$$

If we now set  $M_1 = \rho \Delta x$ , where  $\Delta x$  is the width of particle mass  $M_1$ , then Eq. (6) is just the spatially discretized form of the artificial viscosity part of the one-dimensional version of the vector force equation

$$\rho \frac{d\mathbf{v}}{dt} = -\nabla(p + q), \quad (7)$$

where  $q = \rho(\Delta\mathbf{v})^2/2$  is the nonlinear artificial viscosity with coefficient  $c_2 = 1/2$ , and  $p$  is the usual scalar pressure.

As previously mentioned, the mass interaction rate  $\mathcal{V}$  is somewhat arbitrary. If we estimate that two masses overlap at the rate  $\delta M_2 = \delta M_1 = \rho c_s dt$  then the RHS of Eq. (5) becomes  $\rho c_s \Delta\mathbf{v}_{21} dt/2$  and the linear artificial viscous pressure term is obtained. It is therefore seen that one can introduce any combination of linear and nonlinear artificial viscosity in this manner simply by the choice of the generalized velocity  $\mathcal{V}$  that determines the inelastic collision rate of adjacent masses. Note from this model that the artificial viscosity that acts between any two masses should be turned off when their value of  $\Delta\mathbf{v} > 0$ , since then these masses are not colliding. This has been the principle practiced for a long time, where the definition of ‘‘interaction’’ is extended to discrete grid models of continuum fluids as compression of a zone or part of a zone [10].

It was seen in one dimension that the differencing of the gradient operator resulted automatically from the consideration of the interaction of mass  $M_1$  with its nearest neighbors to the left and right. In more than one dimension what is a nearest neighbor is not so straightforward. In two dimensions using a logically rectangular, staggered, quadrilateral grid there are four nearest neighbors if one considers as a neighbor only the points that lie adjacent to a given point along the logical lines. This gives rise to a five point interaction that loosely resembles the five-point differencing used for discretization of the Laplacian on smooth grids. In the case where one also considers the points that lie diagonally opposite to a given point to also interact one arrives at a nine-point interaction stencil that is more generally used to difference the Laplacian with respect to non-orthogonal quadrilateral grids. Although the edge-centered artificial viscosity developed here cannot be written as the difference form of the continuum Laplacian, this viscosity uses as nearest neighbors only those points that lie along logical lines, with analogy to the five point stencil. Diagonal interactions are not necessarily excluded in principle; however, in this work we have been unable to include these interactions in any generally effective manner that does not degrade the overall quality of the results otherwise obtained.

The major difficulty with the interpretation of the artificial viscosity term as originating from the continuous and differential, inelastic collision of finite volume masses is that we are not dealing with distinct particle masses, but with a continuous fluid that is divided into nodal or point ‘‘particles’’ in a prescribed but somewhat arbitrary manner. If one now proceeds to

use only  $\Delta \mathbf{v} < 0$  between two nodal points to switch on an artificial viscosity, as one would deduce from the above model, one can easily produce erroneous results. For example, one can have the situation of a self-similar, isentropic compression and the above particle model produces irreversible viscous dissipation. This is the essential problem that all artificial viscosity formulations have stumbled over, and which the higher-order Godunov methods [11] are automatically able to overcome. A principal result of this paper is to extend the work of Christiansen [4, 5], which was based on the approximate Riemann solver developed by Dukowicz [12], to the multi-dimensional case for any kind of grid topology. This adds additional restrictions on the strength of the artificial viscous forces such that isentropic compression problems can be solved without unphysical viscous dissipation.

The difficulty with just using the Godunov methods themselves is that one must resort to operator splitting in more than one dimension to solve the associated Riemann problem. This becomes more complicated as more physics (tabulated equations of state, material strength, MHD, etc.) is included in any given model. Artificial viscosity methods are inherently simpler in that the level of numerical complexity does not increase as the number of dimensions and/or the amount of physics included increases.

Finally, we wish to note the following form for the artificial viscosity that is given in the paper by Wilkins [7], but was first presented by Kuropatenko [13]. This is

$$q_{Kur} = \rho \left\{ c_2 \frac{(\gamma + 1)}{4} |\Delta \mathbf{v}| + \sqrt{c_2^2 \left( \frac{\gamma + 1}{4} \right)^2 (\Delta \mathbf{v})^2 + c_1^2 c_s^2} \right\} |\Delta \mathbf{v}|. \quad (8)$$

We refer to this as the Kuropatenko form of the artificial viscosity and label it  $q_{Kur}$ ; note that the mass interaction rate  $\mathcal{V}$  is given by the term inside the curly brackets. In this expression  $\Delta \mathbf{v}$  is the velocity jump across a zone,  $\rho$  and  $c_s$  are the density and speed of sound in this zone (in the Appendix this is somewhat modified);  $\gamma$  is the ratio of specific heats of the material;  $c_1$  and  $c_2$  are constants that multiply the linear and nonlinear artificial viscosity terms, respectively; these are generally set to unity. It is easily seen that Eq. (8) reduces to the linear and nonlinear forms of the artificial viscosity as  $\Delta \mathbf{v} \rightarrow 0$  and  $c_s \rightarrow 0$ , respectively. The above expression is a uniformly valid match to both the linear and nonlinear forms of artificial viscosity as one moves away from the shock front. For this reason it is the basis of the artificial viscosity formulated here.

The origin of the above expression comes from determining the form of the term that must be added to the pressure in front of a steady-state shock in order to achieve the pressure behind the shock, using the jump conditions and, in addition, an ideal gamma-law equation of state. The solution is Eq. (8) where the constants  $c_1 = c_2 = 1$ . In this instance  $\rho$  and  $c_s$  are the density and sound speed ahead of the shock, and  $\Delta \mathbf{v}$  is the velocity jump across it.

### 3. ARTIFICIAL VISCOSITY—ONE-DIMENSION

In one spatial dimension the artificial viscosity forms already given by either Eq. (3) or Eq. (8) are nearly sufficient. The only real difficulty with these expressions is that for uniform compression they do not vanish. This is the problem mentioned earlier with respect to the inelastic collision model of artificial viscosity. We must be able to determine when nodal masses could be arbitrarily redivided into finite size particles with the same average, and thus nodal, velocity as is true for the case of uniform compression, and turn off the artificial viscosity when this occurs.

The most common solution to this problem is to model the artificial viscosity more closely on physical viscosity, which does vanish for uniform compression. To achieve this one redefines a single factor of  $\Delta \mathbf{v}$  in the artificial viscosity as the product  $l_z Q_{ij}$ , where  $l_z$  is the length across a zone and  $Q_{ij}$  is the symmetric strain rate tensor in traceless form. With the generic form of the artificial viscosity, as given by Eq. (3), this becomes

$$\begin{aligned} q_{ij} &= \rho(c_1 c_s + c_2 |\Delta \mathbf{v}|) l_z Q_{ij}, \\ Q_{ij} &= \epsilon_{ij} - \frac{1}{3} \delta_{ij} \nabla \cdot \mathbf{v}, \\ \epsilon_{ij} &= \frac{1}{2} \left( \frac{\partial v_i}{\partial x_j} + \frac{\partial v_j}{\partial x_i} \right), \end{aligned} \quad (9)$$

where  $\epsilon_{ij}$  is the symmetric strain rate tensor and  $\delta_{ij}$  is the kronecker delta function [14]; also,  $q_{ij} = 0$  if  $\Delta \mathbf{v} \geq 0$  across the zone. The tensor  $Q_{ij}$  was derived by requiring that it vanish for rigid rotation and uniform compression [15]. The rest of Eq. (9) is now just a nonlinear, grid dependent form of a coefficient of dynamic viscosity. Although the artificial viscosity is now directional, in one-dimension this has a very simple form. For spherical coordinates  $(R, \theta, \phi)$  where the angles are ignorable so that  $\mathbf{v} = (v(R), 0, 0)$ ,  $Q_{ij}$  becomes

$$Q_{ij} = \left( \frac{2}{3} \right) \begin{pmatrix} \frac{\partial v}{\partial R} - \frac{v}{R} & 0 & 0 \\ 0 & -\frac{1}{2} \left( \frac{\partial v}{\partial R} - \frac{v}{R} \right) & 0 \\ 0 & 0 & -\frac{1}{2} \left( \frac{\partial v}{\partial R} - \frac{v}{R} \right) \end{pmatrix}. \quad (10)$$

(Above and in other instances we sometimes set  $\mathbf{v} = \mathbf{v}(\mathbf{R})$ , where  $\mathbf{R}$  is the radius vector to the point where  $\mathbf{v}$  is defined. By this we indicate a specific functional dependence where  $\mathbf{R}$  is always understood to be nondimensional and  $\mathbf{v}$  has the proper velocity units.) For uniform, self-similar compression  $v = -R$ , and thus  $Q_{ij} = 0$  as desired. Since  $Q_{ij}$  is a proper tensor this property is preserved in all coordinate systems. The force produced by this artificial viscosity is given by  $\nabla_i q_{ij}$  and the associated rate of dissipation by  $q_{ij} : \nabla_j v_i$ . Similar modifications are the basis of most zone-centered forms of the artificial viscosity in more than one dimension.

In implementing the form given as Eq. (9) difficulties may arise due to low-order differencing of the terms that appear in the tensor  $Q_{ij}$ . If two-point formulas are used to evaluate these terms and one of these points is fixed in space, as is the case for a center of convergence, then  $Q_{ij}$  will always vanish in this zone. This is because a discretization using two points is not accurate enough to measure the size of the second derivative of the velocity and always effectively assumes that it is zero. Higher order formulas should be used to difference these terms.

A more recent solution to the uniform compression problem is to retain the ‘‘primitive’’ forms of the artificial viscosity, Eq. (3) or Eq. (8), and realize that what is wanted is to have them vanish when the velocity field is a linear function of the coordinates. Christiansen [4, 5] proposed using a TVD advection limiter [16] in one dimension to achieve this.

Consider a zone in one-dimension delineated by the points ‘‘1’’ and ‘‘2.’’ Suppose that a point labelled ‘‘0’’ lies to the left of ‘‘1,’’ and that a point labelled ‘‘3’’ lies to the right of ‘‘2,’’ so that zones 10 and 32 lie to the left and right, respectively, of the center zone 21. Then the artificial viscosity present in this central zone 21,  $q_{21}$ , is postulated to be

$$q_{21} = q_{Kur,21}(1 - \psi_{21}) \quad \text{if } \Delta v_{21} < 0, \quad (11)$$

and zero otherwise. The limiter  $\psi_{21}$  is given by

$$\psi_{21} = \max[0., \min(.5(r_l + r_r), 2r_l, 2r_r, 1.)]. \quad (12)$$

The quantities  $r_l$  and  $r_r$  that enter the limiter function are given below as the ratios of the discrete spatial derivative of the velocity field on the left and right intervals, respectively, divided by this derivative in the central zone 21

$$r_l = \frac{\Delta v_{32}}{\Delta x_{32}} \bigg/ \frac{\Delta v_{21}}{\Delta x_{21}}, \quad r_r = \frac{\Delta v_{10}}{\Delta x_{10}} \bigg/ \frac{\Delta v_{21}}{\Delta x_{21}}. \quad (13)$$

The limiter appears in Eq. (11) as a linear factor because what is limited is the mass interaction velocity  $\mathcal{V}$  that always enters linearly, and not the velocity difference  $|\Delta \mathbf{v}|$  that enters as a quadratic factor. The enormous advantage the limiters provide is that they always turn the artificial viscosity off when the second derivative of the velocity field is locally zero without directly computing a second difference. Instead, ratios of first differences are used. At the boundaries of the domain where either  $r_l$  or  $r_r$  is missing one can either set the missing ratio to unity or to the other known member for use in Eq. (12). There is found to be little sensitivity to such choices.

We use the expression  $q_{Kur,21}$  in Eq. (11) to indicate that we mean the artificial viscosity form given by Eq. (8) with respect to the interval “21.” This is our recommended form of a one-dimensional artificial viscosity. In one dimension it is always a simple scalar in contrast to the tensor form of Eqs. (9), (10).

#### 4. ARTIFICIAL VISCOSITY—MULTI-DIMENSIONS

We generalize the ideas presented earlier to more than one dimension. Although the discussion will be given in two dimensions, all of the results carry over directly to three dimensions. To help frame this discussion we enumerate the salient properties that a proper artificial viscosity should possess. This is done along the lines of the early work of Schulz [3].

(1) Artificial viscosity must always act to decrease kinetic energy, that is, it must be dissipative (Dissipativity).

(2) Artificial viscosity should vanish uniformly (smoothly) as the velocity field becomes constant (Galilean invariance).

(3) Artificial viscosity should vanish for a uniform contraction and/or a rigid rotation (Self-similar motion invariance).

(4) Artificial viscosity should have no effect along a wave front of constant phase. This is because the velocity component tangential to a shock front is continuous in the limit of arbitrary grid refinement in this direction (Wave front invariance).

(5) The artificial viscous force should go to zero continuously as compression vanishes and expansion develops, and remain zero for the latter. Compression and expansion must be defined in some relevant context (Viscous force continuity).

Before we can judge the merits of a particular form of artificial viscosity we must first be certain that it is dissipative: that is, an artificial viscosity and not a false pressure term that can act to increase as well as decrease kinetic energy and thus give rise to wave motion. To guarantee that an intended form of artificial viscosity is always dissipative is a nontrivial point that says much about the functional form of the artificial viscosity itself. To ensure this we must examine the internal energy equation and how dissipation is achieved given forces

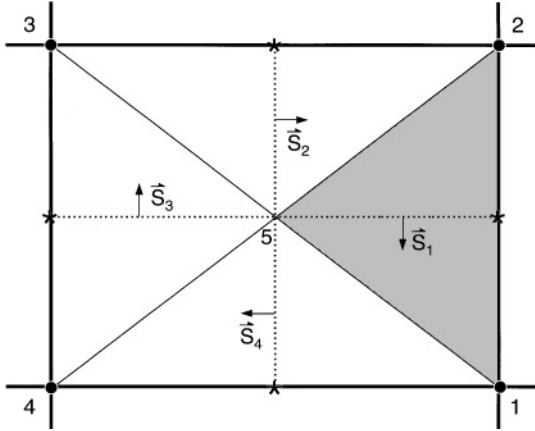


**FIG. 1.** Quadrilateral zone: solid interior lines delineate triangular subzones; dotted lines form the median mesh.

that are discretized via a control volume method along the median mesh. As a prerequisite for this development it is necessary to present the basics of the control volume differencing that is utilized.

#### 4.1. Control Volume Differencing/Median Mesh Forces

In the general case where only a postulated form of the artificial viscosity is specified we need to answer two questions: First, given conservation of total energy, what is the form of the equation for internal energy with specified forces; and second, under what conditions do these forces result in positive-definite work? The first question can always be answered. This is given in the framework of what we call “compatible” or “mimetic” discretization of the equations [2, 17]. We give enough background for our purposes but refer otherwise to the discussion of these themes in a broader context [2, 19]. We note, however, that in the compatible formulation of difference equations on a staggered spatial grid the force on the points and the work done with respect to the zones are composed of the same sub-pieces of force; these are simply manipulated in different manners as is now illustrated.

To be explicit, consider Fig. 1 where a quadrilateral zone is shown that is subdivided by solid lines to form triangular subzones. The coordinates of the center point labelled as “5” are determined as the average of the coordinates of the points that form the quadrilateral. The solid lines that compose the boundary of the quadrilateral form the “coordinate-line” mesh. The dotted lines that connect point “5” to the midpoints of each side of the quadrilateral and bisect each subtriangle form the “median” mesh. The vectors labelled  $\vec{S}_i$ , where  $i = 1 \dots 4$ , are the normals to these lines with magnitudes that are equal to their areas. It is along the median mesh that we will compute the forces that are due to the artificial viscosity, and thus we must explain how these forces and the work they produce are to be computed with respect to this mesh.

Suppose that there exists a tensor  $\bar{\bar{Q}}_z$  of arbitrary origin that is piecewise constant inside zones with logical index  $z$ . Then using control volume differencing the momentum equation at any point  $p$  can be written as

$$M_p \frac{d\mathbf{v}_p}{dt} = \oint_{S_p} \bar{\bar{Q}} \cdot d\mathbf{S}, \quad (14)$$

where on the LHS  $M_p$  is the mass, and  $\mathbf{v}_p$  is the velocity, of the point  $p$ . The force on the RHS of Eq. (14) is evaluated along the closed contour  $S_p$  of the median mesh about point  $p$ , and obtains two piecewise constant contributions from each zone adjacent to this point. We are next concerned with the exact specification of these force contributions.

The zone shown in Fig. 1 contains forces labelled as  $\mathbf{f}_i$ , where  $i = 1 \dots 4$ . These are computed along the median mesh by the dot product of this tensor with the respective vectors  $\mathbf{S}_i$ , or  $\mathbf{f}_i = \bar{\mathcal{Q}}_z \cdot \mathbf{S}_i$ . These forces now individually act upon their adjacent two points with opposite signs consistent with Newton's third law. Thus, if we allocate the force  $\mathbf{f}_1$  to the sum of forces computed on point 1 with a + sign, then it must also be added to the sum of forces computed on point 2 with a - sign. The total force on any given point is just the sum of all forces allocated to it from all zones that lie adjacent. Therefore, point 1 accumulates forces  $\mathbf{f}_1$  and  $\mathbf{f}_4$  from the given zone  $z$  in Fig. 1, with the signs of these forces determined by the conventions chosen. As will be seen, these signs can be found by simple logic. This completes the determination of the contribution to the momentum equation of the forces  $\mathbf{f}_i$  resulting from the tensor  $\bar{\mathcal{Q}}_z$ , which is specified inside the zone in some manner. The acceleration of the points can now be computed using these forces, and whatever other forces, are present.

An important result of the compatible formulation of the equations of hydrodynamics is that the work performed by the forces  $\mathbf{f}_i$  can be computed with respect to the zone  $z$  in which they originate simply as  $-\mathbf{f}_i \cdot \mathbf{v}_p$ , where  $\mathbf{v}_p$  is the velocity of the point  $p$  that the force  $\mathbf{f}_i$  acts upon [2]. Thus the rate of work done by the force  $\mathbf{f}_1$ , computed with respect to the part of the median mesh  $\mathbf{S}_1$  and allotted to point 1 with a + sign and to point 2 with a - sign, is given by the term  $-\mathbf{f}_1 \cdot (\mathbf{v}_1 - \mathbf{v}_2) \equiv -\mathbf{f}_1 \cdot \Delta \mathbf{v}_{12}$ . If we sum all four such contributions along the median mesh the equation for the evolution of internal energy in zone  $z$  becomes

$$M_z \frac{de_z}{dt} = \sum_{i=1}^4 -\mathbf{f}_i \cdot \Delta \mathbf{v}_i, \quad (15)$$

where  $M_z$  is the zone mass and  $e_z$  is its specific internal energy. The indicated sum is cyclic so that  $\Delta \mathbf{v}_i \equiv \mathbf{v}_i - \mathbf{v}_{i+1}$ , and when  $i = 4$  we identify point  $i + 1 \rightarrow 1$ .

For the forces  $\mathbf{f}_i$  originating from the tensor  $\bar{\mathcal{Q}}_z$  it can be shown that the RHS of Eq. (15) reduces to the usual discrete control volume form of the heating term  $Q_{k,l} : \nabla_k v_l$  integrated over the volume of the zone  $z$  [2]. (The dummy indicies  $k, l$  are summed over either two or three spatial dimensions.) Next, if we specify that the force  $\mathbf{f}_i$  originates from a scalar pressure  $p_z$  that is constant in zone  $z$  then,  $\mathbf{f}_i = p_z \mathbf{S}_i$ . Since the pressure is positive it acts to expand any given zone and the force  $\mathbf{f}_1 = p_z \mathbf{S}_1$  should be applied to point 1 with a + sign and to point 2 with a - sign, given the direction of the median mesh vector  $\mathbf{S}_1$  that is indicated in Fig. 1. Thus from Eq. (15) the work term due to  $\mathbf{f}_1$  is  $-p_z \mathbf{S}_1 \cdot (\mathbf{v}_1 - \mathbf{v}_2)$ . When these four zone contributions are summed they reduce to the discrete control volume form of  $-p_z dV_z$ , where  $dV_z$  is the rate of change of the volume of the zone  $z$  [19]. Thus we have the important result that

$$dV_z \equiv V_z (\nabla \cdot \mathbf{v})_z = \sum_{i=1}^4 \mathbf{S}_i \cdot \Delta \mathbf{v}_i. \quad (16)$$

Normally, when the divergence of the velocity of a zone,  $(\nabla \cdot \mathbf{v})_z$ , is positive the artificial viscosity in that zone is turned off. Next, it is shown how to generalize this result to an edge-centered artificial viscosity, and to ensure that the work performed by it is always positive.

#### 4.2. Dissipativity

Unlike the case in one dimension, in two or more dimensions it is necessary to consider whether the form of the artificial viscosity is centered in a zone, or is along an edge as was initially envisioned by Schulz [3]. A zone-centered artificial viscosity is piecewise constant in a zone, while an edge-centered artificial viscosity is piecewise constant in each of the four subzonal triangles shown in Fig. 1, or in general, in every subtriangle along every coordinate edge of an associated zone that can contain any number of sides.

For the case of a zone-centered, scalar artificial viscosity,  $q$ , that enters the equations in the same way as the pressure, the work done is simply  $-q dV_z$ , where  $dV_z$  is the rate of change of the volume of a zone that is given in discrete form by Eq. (16). Since  $q$  is positive and nonzero only for  $dV_z$  less than zero the work done is always positive as desired. We now use this example to generalize the zone compression criteria to the individual edges of a zone. Since  $(\nabla \cdot \mathbf{v})_z < 0$  for a zone to be under compression, for the  $i$ th triangular subzonal edge of zone  $z$  to be under compression we postulate the condition

$$\mathbf{S}_i \cdot \Delta \mathbf{v}_i < 0. \quad (17)$$

The quantities  $\mathbf{S}_i \cdot \Delta \mathbf{v}_i$  are seen from Eq. (16) to be the individual edge contributions to the divergence of the velocity defined in zone  $z$ .

As noted, the internal energy equation, Eq. (15), is valid for forces  $\mathbf{f}_i$  that are of completely general origins. From this equation we see that if the force  $\mathbf{f}_i$  points antiparallel to  $\Delta \mathbf{v}_i$ , then this force does positive-definite work. This is a sufficient, though not necessary, condition for dissipativity that our form of artificial viscous forces are constructed to obey. This observation itself is enough to guarantee that our edge-centered viscous forces,  $\mathbf{f}_i$ , are always dissipative. However, this condition will be seen to automatically incorporate Eq. (17) that defines edge compression. Then it becomes simple to specify the correct signs to be used in allocating the viscous forces along each zone edge to the momentum equation of its two respective points. This we do after a brief digression to consider the important subject of limiters, which is also necessary for the complete specification of our artificial viscosity.

#### 4.3. Viscosity Limiters in Multi-dimensions

The velocity gradient limiter that was given in one dimension is now generalized to multi-dimensions. This is done with respect to the coordinate edges of zones of arbitrary shape. The edges to the left and right of a given edge are automatically defined for a logically constructed grid. We now give a general prescription for the velocity derivative ratios  $r_l$  and  $r_r$  of Eq. (13) in multi-dimensions. It is then shown how, in conjunction with Eq. (12) for the limiter function  $\psi_i$  along the  $i$ th edge, the artificial viscosity can be made to vanish for uniform compression, rigid rotation, and along a front of constant phase.

Consider an edge labelled  $i$  of a grid in two dimensions. From its two defining endpoints we know  $\Delta \mathbf{x}_i$ , its vector length, and  $\Delta \mathbf{v}_i$ , the difference in the velocity along this length;  $\widehat{\Delta \mathbf{x}}_i$  and  $\widehat{\Delta \mathbf{v}}_i$  are the unit vectors that point in the direction of the edge vector length and the velocity difference, respectively. In general, the vectors  $\Delta \mathbf{x}_i$  and  $\Delta \mathbf{v}_i$  are in different directions. Thus, what is known along this edge is a particular slice of the tensor gradient of the velocity field,  $\nabla_i v_j$ . We want to compare this slice of the velocity gradient to another one that lies to the left and right of this edge; these edges are labelled  $i + 1$  and  $i - 1$ , respectively. However, we can only compare commensurate objects. To this end we form

the dot product of the velocity difference along edge  $i$  with that along edge  $i + 1$ , and divide this by the dot product of the vector length along edge  $i$  with that along edge  $i + 1$ . This operation projects the slice of the velocity gradient tensor known along edge  $i + 1$  to that known along edge  $i$ . Next, this entire quantity is divided by the square of the velocity difference along edge  $i$  over the square of the vector length along edge  $i$ . This latter step is the exact analog of the first, only this time performed with respect to the edge  $i$  itself. This entire operation yields the quantity  $r_{l,i}$ . Performing the same procedure with respect to the right edge  $i - 1$  yields  $r_{r,i}$ . These are the left and right velocity derivative ratios needed for the one-dimensional limiter given by Eq. (12). They are conveniently written as

$$r_{l,i} = \frac{\Delta \mathbf{v}_{i+1} \cdot \widehat{\Delta \mathbf{v}}_i}{\Delta \mathbf{x}_{i+1} \cdot \widehat{\Delta \mathbf{x}}_i} \bigg/ \frac{|\Delta \mathbf{v}_i|}{|\Delta \mathbf{x}_i|}, \quad r_{r,i} = \frac{\Delta \mathbf{v}_{i-1} \cdot \widehat{\Delta \mathbf{v}}_i}{\Delta \mathbf{x}_{i-1} \cdot \widehat{\Delta \mathbf{x}}_i} \bigg/ \frac{|\Delta \mathbf{v}_i|}{|\Delta \mathbf{x}_i|}. \quad (18)$$

It is easily seen that these quantities reduce to those given by Eq. (13) in the one-dimensional case. Note that as the velocity field goes to a constant the ratios given above become indeterminate,  $(0/0)$ . Care must thus be taken in coding these objects (see the Appendix). The purpose of a viscosity limiter is to eliminate linear gradients of the velocity field. A constant velocity field is eliminated by the direct dependence of the artificial viscosity on  $\Delta \mathbf{v}_i$  itself. The only other restriction on the above quantities is that the vector  $\widehat{\Delta \mathbf{x}}_i$  not be at exactly a right angle with respect to either  $\Delta \mathbf{x}_{i+1}$  or  $\Delta \mathbf{x}_{i-1}$ .

For a logical grid such as that shown in Fig. 2 the concept of left and right with respect to a given edge is taken care of trivially by the logical indexing. For an unstructured grid the definition of left and right is generalized by considering the nearest neighbors to the respective endpoints of a given edge. Thus, the nearest neighbors to the left endpoint all contribute candidate left edges and thus  $r_{l,i}$ 's, except that for accuracy we require that the

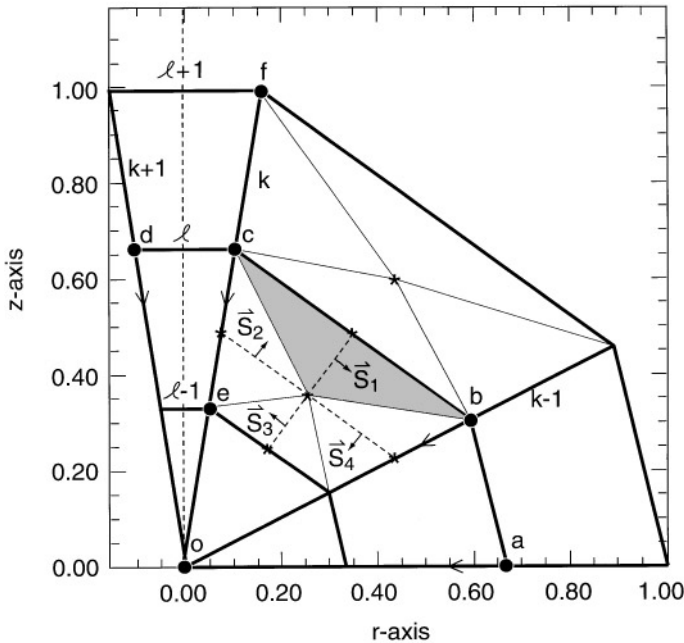


**FIG. 2.** Logical  $k - l$  grid. Points  $a \cdots d$  are on a surface of constant major radius and phase.  $\mathbf{S}_1 \cdots \mathbf{S}_4$  are vectors that define the median mesh of the central zone.

angle between these edges and the given  $i$ th edge be less than  $90^\circ$ . To find the  $r_{l,i}$  to use in the limiter formula for  $\psi_i$  we then simply choose the maximum value of these possibilities, and likewise for  $r_{r,i}$ .

Although uniform compression has been discussed in the one-dimensional case, in two dimensions and in cylindrical coordinates  $(r, z)$  the velocity field has the form  $\mathbf{v} = (-r, -z)$  for this motion: for rigid rotation  $\mathbf{v} = (z, -r)$ . Thus it is seen that uniform compression and rigid rotation are conjugate motions. What we require is an artificial viscosity that vanishes when the velocity field is a linear function of the coordinates. We call this “self-similar motion invariance.” Next, consider Fig. 2 where a grid is shown that could correspond to either cylindrical or Cartesian geometry with points  $a \cdots d$  that lie on a line of constant major radius. For a velocity field that is directed radially inward our fourth criteria says that no artificial viscous forces should act between the points  $a \cdots d$  that lie on a common phase front. That this should be true is obvious since along these points there are no discontinuities in any variables. So along a phase front the artificial viscosity should dissipate no kinetic energy; we refer to this property as “wave front invariance.” Next it is shown that our new limiter prescription turns off the artificial viscosity for these conditions.

When the values of the velocity derivative ratios given by Eq. (18) are both greater than or equal to unity, the limiter  $\psi_i = 1$  and the artificial viscosity is turned off along the  $i$ th edge. From the previous discussion, a velocity field that is a linear function of the coordinates has  $\Delta \mathbf{v}_i = -\Delta \mathbf{x}_i$  and  $\Delta \mathbf{v}_i = \Delta \mathbf{x}_{\perp,i}$ , for uniform compression and rigid rotation, respectively. Then it is readily seen from Eq. (18) that  $r_{l,i} = r_{r,i} = 1$ ; this is true regardless of the spacing of the grid points.

Suppose there is convergent radial flow as indicated in Fig. 2. Then we want to show that the given artificial viscosity will turn off along a front of constant phase, such as that on which the points  $a \cdots d$  lie. Along any edge aligned with a phase front  $\Delta \mathbf{v}_i$  is parallel to  $\Delta \mathbf{x}_i$ . Thus in computing the quantities given by Eq. (18) the angular factors that arise from terms such as  $\Delta \mathbf{x}_{i+1} \cdot \widehat{\Delta \mathbf{x}}_i$  and  $\Delta \mathbf{v}_{i+1} \cdot \widehat{\Delta \mathbf{v}}_i$  cancel when these terms are divided to obtain  $r_{l,i}$  or  $r_{r,i}$ . One is left with the ratios of positive quantities,  $(\Delta v / \Delta x)_{i+1}$  to  $(\Delta v / \Delta x)_i$ , that are all equal for any phase front. Thus, both  $r_{l,i}$  and  $r_{r,i}$  will be unity, resulting in  $\psi_i = 1$ , and the viscosity on this edge will vanish. This occurs independently of the angular distribution of the points that lie on a phase front.

The complete limiter specification requires a brief discussion of how  $r_{l,i}$  and  $r_{r,i}$  are to be set when one of them lies outside of the problem domain as will occur at every boundary. In Fig. 2 is shown two types of reflecting boundaries. Along the  $z$ -axis the reflecting boundary is placed through the center of the zone. For the edge “ $dc$ ” it is easy to show from Eq. (18) that  $r_{l,i} = r_{r,i}$ . For a reflecting boundary along a coordinate edge, as shown for the  $r$ -axis in Fig. 2, the magnitudes of the vectors divide out in Eq. (18) and  $r_{r,i}$  along the edge  $ba$  becomes simply the ratio of the dot products of the appropriate unit vectors. For an edge such as  $eo$  next to a center of convergence, or  $fc$  next to an outer boundary, we simply set the unknown member equal to unity. Or alternatively, one can set it to the known member as in the reflective boundary case. We find that the results show little sensitivity to these choices.

#### 4.4. Edge-Centered Artificial Viscosity

We now have the pieces that are needed to construct an edge-centered artificial viscosity that will satisfy all of our stated criteria. Aside from “dissipativity,” of the five criteria that any proper artificial viscosity should conform to, “self-similar motion invariance” and

“wave front invariance” are taken care of by the limiter prescription computed with respect to each edge. We are now concerned with the remaining two: “viscous force continuity” and “Galilean invariance.”

The starting point for our edge-centered artificial viscosity is the scalar Kuropatenko form, denoted as  $q_{Kur,i}$  along an  $i$ th edge, as given by Eq. (8). After endowing this form with “directionality,” we will postulate that this tensor form, denoted as  $\bar{q}_{i,z}$ , is present in the  $i$ th triangular subzone associated with every edge of a given zone  $z$  as depicted in Fig. 1, and gives rise to a viscous force  $\mathbf{f}_i$  that is computed along the median mesh as,  $\mathbf{f}_i = \bar{q}_{i,z} \cdot \mathbf{S}_i$ . (Note that now the tensor  $\bar{q}_{i,z}$  is subzonal.)

The problem of directionality is resolved by noting, from the arguments concerning inelastic collisions of masses that led to Eq. (5), that the viscous force should be in the  $\Delta \mathbf{v}_i$  direction; in addition, as was noted from Eq. (15), this guarantees that the viscous force performs positive-definite work. Next we require that the artificial viscosity should be a symmetric tensor that is nonzero only when the edge in which it is defined is under compression, as stated by the inequality given in Eq. (17). Thus we conclude that the tensor form along each edge should consist of the following pieces: first, the scalar factor  $q_{Kur,i}$ , and directionality specified by the projection operator that is defined by the direct product of the unit vector of the difference of the velocities along an edge,  $\widehat{\Delta \mathbf{v}_i}$ , with itself. This is written as  $\widehat{\Delta \mathbf{v}_i} \widehat{\Delta \mathbf{v}_i}$ . (We always use dyadic notation to denote the direct product of two unit vectors.) Collecting these pieces along with the edge limiter function, the tensor form for our edge-centered artificial viscosity along edge  $i$  of zone  $z$  can be written as

$$\bar{q}_{i,z} = q_{Kur,i} (1 - \psi_i) \widehat{\Delta \mathbf{v}_i} \widehat{\Delta \mathbf{v}_i} \quad \text{if } \Delta \mathbf{v}_i \cdot \mathbf{S}_{i,z} < 0, \text{ else } \bar{q}_{i,z} = 0. \quad (19)$$

For the limiter  $\psi_i$  we still use Eq. (12), but the functions that enter it are the left and right velocity derivative ratios,  $r_{l,i}$  and  $r_{r,i}$ , with respect to the  $i$ th edge of a zone as given by Eq. (18).

Evaluating the piece of the viscous force along the  $i$ th segment of the median mesh,  $\mathbf{f}_i$ , of a zone  $z$  due to  $\bar{q}_{i,z}$  we have

$$\mathbf{f}_i = \bar{q}_{i,z} \cdot \mathbf{S}_{i,z} = q_{Kur,i} (1 - \psi_i) (\widehat{\Delta \mathbf{v}_i} \cdot \mathbf{S}_{i,z}) \widehat{\Delta \mathbf{v}_i}, \quad (20)$$

if  $\Delta \mathbf{v}_i \cdot \mathbf{S}_{i,z} < 0$ , otherwise  $\mathbf{f}_i = 0$ , where the on/off condition is a consequence of Eq. (17). Note that because the on/off switch also appears as a factor in Eq. (20), the force  $\mathbf{f}_i$  depends continuously on this quantity and thus our fifth criterion “viscous force continuity” is satisfied. The second criterion “Galilean invariance” follows because the form of  $q_{Kur,i}$ , that makes up the scalar kernel of our artificial viscosity, is an explicit function of  $\Delta \mathbf{v}_i$ . Now since the viscous force that acts between points 1 and 2 has direction  $\mathbf{f}_1 \sim -\widehat{\Delta \mathbf{v}_1}$ , and since  $\Delta \mathbf{v}_1 = (\mathbf{v}_1 - \mathbf{v}_2)$ , from Eq. (15),  $\mathbf{f}_1$  must be applied to point 1 with a + sign and to point 2 with a – sign in order to reduce the size of  $\Delta \mathbf{v}_1$ , and thus be dissipative (see also the discussion given in the Appendix). It is important to note that since the artificial viscous forces originate from  $\bar{q}_{i,z}$ , that is not constant throughout a zone, that it is only by means of the general form of Eq. (15) that the rate of work performed by these forces can be computed. Unlike in the case where  $\bar{Q}_z$  was constant in a zone, no expression for the undiscretized, intensive heating rate resulting from the tensor  $\bar{q}_{z,i}$  exists.

The edge-centered viscosity just given uses a switch that is not the actual rate of compression of any volume but sums to the rate of change of the zone volume, as previously noted. To see that this switch is actually superior to using  $dV_z$ , or equivalently  $(\nabla \cdot \mathbf{v})_z$ ,

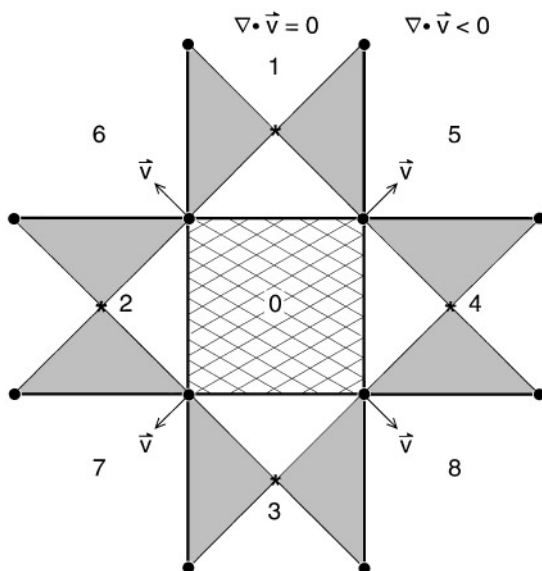


**FIG. 3.** Square grid with velocity vectors after one timestep. Energy source in hatched zone 0. In shaded triangular regions the edge artificial viscosity turns on.

of an entire zone as an on/off criteria, consider the situation shown in Fig. 3. This figure shows an energy source in the central zone labelled 0, and the velocity field is shown after one timestep. At this time  $(\nabla \cdot \mathbf{v})_z$  is zero for the zones labelled  $1 \cdots 4$  and the viscosity is thus zero in these zones using this criteria. However, the edge viscosity will be present in the shaded subtriangular regions of these zones. The artificial viscosity should obviously be on in all zones surrounding the energy source.

*4.4.1. Comparison to the work of Schulz.* It is interesting to contrast our edge-centered viscosity formulation to that of Schulz [3] who also listed “self-similar motion invariance” and “wave front invariance” as criteria necessary for a suitable artificial viscosity, and his formulation does satisfy these conditions. This was achieved by changing the form of the artificial viscosity from  $(\Delta \mathbf{v}_i)^2$  (Schulz utilized only the projection of  $\Delta \mathbf{v}_i$  along the edge direction  $\widehat{\Delta \mathbf{x}}_i$ , and there was no linear term) to the product of  $|\Delta \mathbf{v}_i|$  times  $|\Delta \mathbf{v}_{2,i}|$ , where  $|\Delta \mathbf{v}_{2,i}|$  is the magnitude of the second difference of the velocity field along the logical line of the  $i$ th edge. (The sign of  $\Delta \mathbf{v}_i \cdot \widehat{\Delta \mathbf{x}}_i$  was used as the compression switch, and  $\widehat{\Delta \mathbf{x}}_i$  as the force direction.) This results in a primitive form of limiter that turns the artificial viscosity off along a phase front for radially symmetric flow when the  $k$ -lines shown in Fig. 2 are spaced with equal angles. This also makes the artificial viscosity vanish for uniform compression and rigid rotation. By using the second difference of the velocity field it is no longer clear that this viscosity will give the same zone compression independent of shock strength. In addition, the use of second differences results in much increased high spatial frequency numerical noise relative to the limiter procedure, which only involves ratios of first differences.

As pointed out by Schulz, his edge-centered viscosity is not symmetric. However, he did try a symmetric form based on  $\widehat{\Delta \mathbf{v}}_i$  of an edge [18]. He noted that this did give a smoother hydrodynamics algorithm than his previous asymmetric form. However, he abandoned it because he was also trying to control spurious grid distortion with his artificial viscosity, as

well as to resolve shocks. We demonstrate that spurious grid distortion is better controlled by other means [19].

#### 4.5. Zone-Centered Artificial Viscosity

Since zone-centered artificial viscosity treatments have been used more widely in the past than edge-centered ones, we briefly consider this formulation. We consider first the zone-centered, scalar form of the artificial viscosity formulated by Wilkins [7]. He uses the generic form,  $q_{gen}$ , given as Eq. (3) and splits the factor  $\Delta v$  into two multiplicative factors  $l^*$  and  $\nabla \cdot \mathbf{v}^*$ . These new quantities are defined by first finding the shock direction across the zone. This is usually determined as the direction associated with the average pressure gradient of the zone points. This unit direction we label as  $\hat{c}$ . The next step is to project the velocity at the zone points in this direction so that  $\mathbf{v}^* \equiv (\hat{c} \cdot \mathbf{v})\hat{c}$ ; then,  $\nabla \cdot \mathbf{v}^*$  is simply the divergence of this projected velocity field, which defines the rate of compression in this direction. (Wilkins refers to this quantity as  $ds/dt$  [7]; it can be equivalently written as  $\epsilon_{ij} : c_i c_j$ , where  $\epsilon_{ij}$  is the symmetric strain rate tensor defined earlier in Eq. (9), see also [20].) The length  $l^*$  is the effective length through the zone relative to the direction  $\hat{c}$ , which can be determined in more than one manner [7, 21]. The quantity  $\nabla \cdot \mathbf{v}^*$  is also used as the compression switch in this formulation, so this form of artificial viscosity turns off in a continuous manner.

The first difficulty with the Wilkins formulation is that it does not result in a viscous force that vanishes on a front of constant phase, and thus does not take out all non-shock components as was intended. This is because it is still a scalar. A scalar viscosity acts normal to all edges of the median mesh and thus produces forces and consequent dissipation between points that are common to a single convergent phase front.

Since the unit vector  $\hat{c}$ , defined in the zone center, is perpendicular to the velocity difference  $\Delta \mathbf{v}$  along a front of constant phase, this difficulty can be remedied by allowing the Wilkins viscosity, now labelled  $q_{gen}^W$ , to have the simple directional form  $q_{gen}^W \hat{c} \hat{c}$ . Now the force along an edge is given by  $q_{gen}^W (\hat{c} \cdot \mathbf{S}_i) \hat{c}$ , and the dissipation due to this force along a front of constant phase vanishes. A zone-centered viscosity of this form has been employed by Burton [20].

Neither of the above formulations vanishes for uniform compression or rigid rotation. To remedy this difficulty one may choose the tensor artificial viscosity form given by Eq. (9) since, as noted previously,  $Q_{ij}$  has this property. However, this formulation will not yield a viscosity that vanishes along a phase front. For these reasons we prefer the flexibility that is afforded by an edge-centered artificial viscosity, although, as has been discussed by Margolin [23], one can utilize an edge-centered formulation to derive a zone-centered viscosity as a special case. Then this zone-centered viscosity will have the same properties as the edge-centered one from which it was derived except that it does not respond to hourglass distortion.

## 5. NUMERICAL SENSITIVITIES

The edge-centered artificial viscosity presented here has been used as a part of an advanced Lagrangian hydrodynamics algorithm [2, 19, 22]. Thus a large variety of results has been presented that illustrate its effectiveness within a wider context. For instance, because there are no zone specific factors, this viscosity is used without need of any modification for problems that preserve a special symmetry [22]. In all of these publications the linear and nonlinear viscosity coefficients,  $c_1$  and  $c_2$ , are set to unity and the limiters are on. In this

section we exhibit the sensitivity of this artificial viscosity to its coefficients, and illustrate the effectiveness of the limiters, for shock wave and adiabatic flow. All problems are run with an ideal gas,  $\gamma = 5/3$ , equation of state. All change in internal energy is computed compatibly and thus total energy is conserved to roundoff error.

The first problem shows that our edge-centered artificial viscosity will turn off for a velocity field corresponding to uniform compression on a grid whose points are distributed in a random manner. In Fig. 4(a) is shown an initially square, logical grid in cylindrical

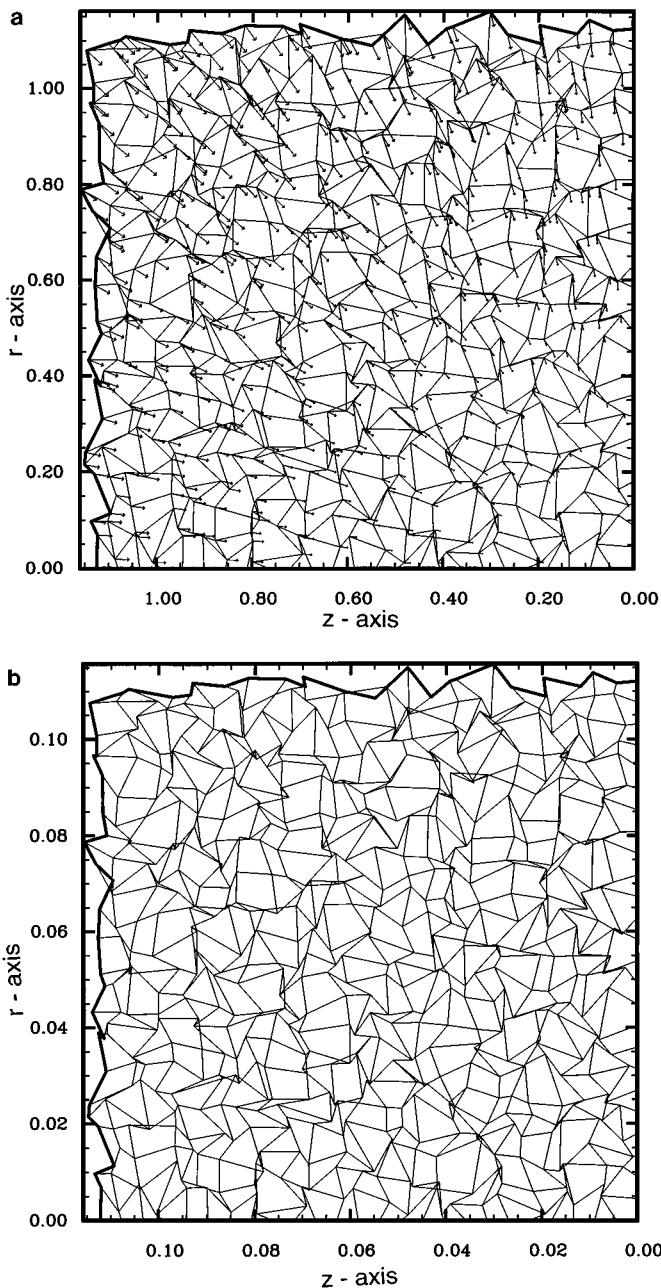


**FIG. 4.** (a) Randomized initial grid with initial velocity field  $\mathbf{v} = (-r, -z)$  in cylindrical coordinates. (b) Final grid after 1000 fold volume compression.

coordinates that has been randomized with a factor of 0.8 times the initial grid spacing. The velocity field is initialized to minus the value of the grid point coordinates, and is shown as the vectors in this figure. The initial density is unity and the initial pressure is zero. Since the initial speed of sound is zero, the timestep of the calculation is constrained by requiring that no zone decrease in volume by more than one percent on a cycle. In Fig. 4(b) the grid is shown after the coordinates have decreased by a factor of ten (about 450 cycles); the density has increased by just over a factor of 1000 and is flat, as it should be for the specified initial velocity field. The artificial viscosity has remained zero to round-off error. This shows that for a velocity field that corresponds to self-similar motion the limiter formulation given here is independent of the grid topology. We note that when this artificial viscosity is implemented in cylindrical geometry all hoop stress, or body force, terms are omitted since this is still considered to be a postulated force; these extra terms only produce unwanted numerical complications.

Next we consider Noh's spherical problem calculated in cylindrical geometry [5, 24]. This problem has been used extensively to illustrate the difficulties of preserving spherical symmetry in cylindrical geometry [22]. Initially the velocity is directed radially inward with a magnitude of  $-1.0$ , the density is unity, and the internal energy is zero. We show in Fig. 5 as the solid curve our standard numerical result for the density as a function of major radius at the time of 0.6 using a 201  $l$ -line resolution, and with the viscosity coefficients  $c_1 = c_2 = 1$ . The dotted curve that lies just below it corresponds to the same parameters except that  $c_1 = c_2 = 2$ . The dash-dot curve that lies just above it, and shows some ringing behind the shock front, is the result for  $c_1 = c_2 = 0.5$ . As seen, these curves are all close together and agree well with the analytic result of a flat density equal to 64.0 inside the shock region that has a radius of 0.2 at time 0.6, except for the usual wall heating problem that is discussed at the end of this section. The limiters here are on; however, we have tried other forms in place

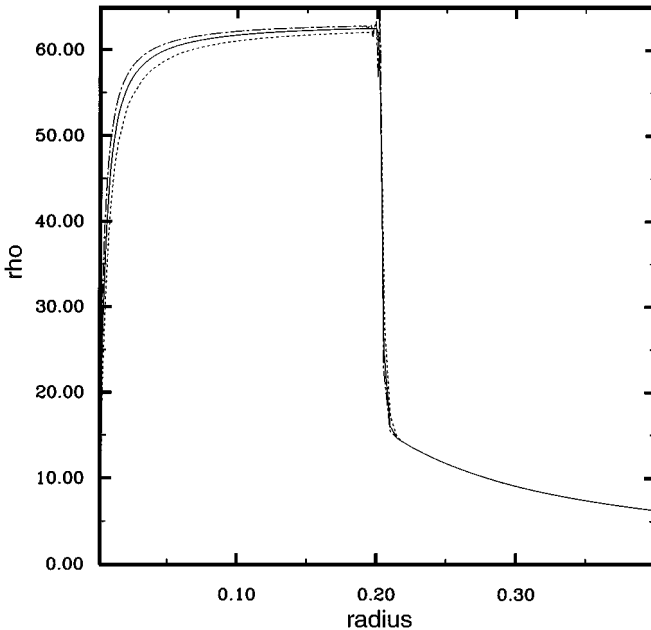


**FIG. 5.** Noh's problem-density versus major radius at time 0.6: solid curve is the standard result  $c_1 = c_2 = 1$ ; dotted curve,  $c_1 = c_2 = 2$ ; dash-dot curve,  $c_1 = c_2 = 0.5$ .

of the limiter function  $\psi_i$ , as given by Eq. (12). In particular, all of the additional forms given in the paper by Benson and Schoenfeld [5] result in oscillations behind the shock for this problem with  $c_1 = c_2 = 1$ . These limiter functions just have different dependencies on  $r_l$  and  $r_r$ . Although they all turn the artificial viscosity off when the velocity field is a linear function of the spatial coordinates, they result in different values depending on the magnitude of the second spatial derivative of the velocity field. The criterion for the best advection scheme is that the limiter allow the least amount of diffusion of the advected quantity. For a viscosity limiter the criterion is that the limiter be a function that is as smooth as possible with respect to its arguments  $r_l$  and  $r_r$ . This criterion is necessary to avoid spurious oscillation in the solution behind the shock front.

The Noh problem is also used to illustrate the substantial errors that can occur when the artificial viscosity is allowed to act along a front of constant phase. (In all following results the viscosity coefficients  $c_1$  and  $c_2$  are set to unity unless specified otherwise.) In Fig. 6 the solid curve is again our standard result for the density as a function of radius. The dotted line just below it is the result obtained when the limiters along the radially outward  $k$ -lines (cf., Fig. 2) are turned off; however, those along the  $l$ -lines that form constant phase surfaces for this problem are still on. It is seen that this results in only a slightly more dissipative answer. The three dashed curves in this figure give results with all limiters off, and for the indicated angular zoning. For the case of only three  $k$ -lines the angle separating them is  $45^\circ$  and the result is essentially unrecognizable. As seen, the error does decrease as more  $k$ -lines are added (at  $5^\circ$  there are 19  $k$ -lines); however, this is a physical problem that has no angular dependence. Note that because of the overheating the speed of the shock front is too fast for the cases indicated by the dashed lines. When the viscosity is turned off along the  $l$ -lines our results show no sensitivity to angular zoning. The solid and dotted curves in this figure were from runs using three  $k$ -lines. This difficulty is not specific to edge-centered

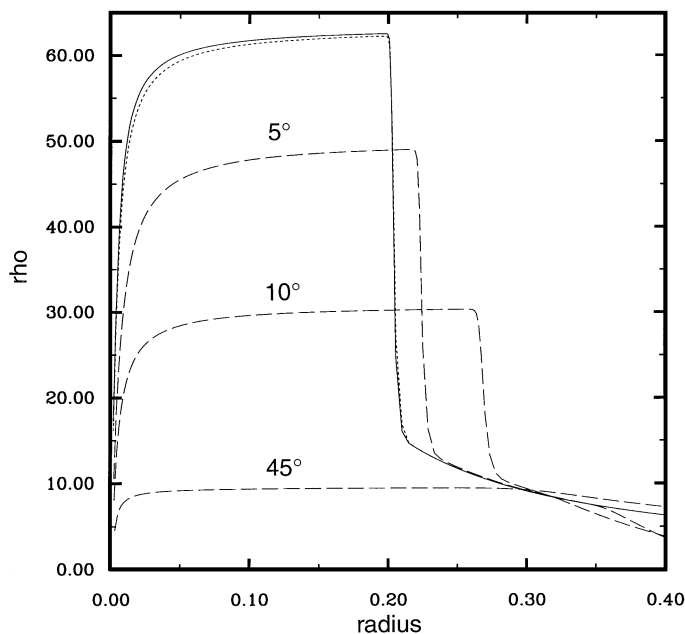


**FIG. 6.** Noh's problem—density versus major radius at time 0.6: solid curve is standard result—all limiters on; dotted curve, limiters off only with respect to  $k$ -lines; dashed curves, all limiters off ( $45^\circ$ ,  $10^\circ$ ,  $5^\circ$ ) angular zoning.

viscosity and will occur with just as much virulence for zone-centered forms that act along a front of constant phase.

The preceding example shows why artificial viscosity is qualitatively more difficult to formulate in two or more dimensions than in one dimension. Limiters on or off along the  $k$ -lines in the above example correspond to the differences one expects in one dimension, and these are seen to be relatively small. However, when artificial viscosity is present along a phase front in two or more dimensions potentially huge errors can arise.

The Coggeshall adiabatic compression problem [25] tests the ability of an artificial viscosity to distinguish between adiabatic and shock compression in the case where there is no obvious one-dimensional symmetry. This two-dimensional problem involves adiabatic compression only and has an analytical solution. The setup consists of a quarter of a sphere of unit radius zoned with 11 equally spaced radial  $k$ -lines ( $9^\circ$  increments) and 101 equally spaced lateral  $l$ -lines in a cylindrical  $(r, z)$  coordinate system. The initial velocity at the grid points is given in terms of their coordinate values as  $\mathbf{v} = (-r, -z/4)$ , and the initial density is unity. The specific internal energy of a zone is given as  $(3\bar{z}/8)^2$ , where the average coordinate  $\bar{z}$  of a quadrilateral zone is taken as the geometric mean of the  $z$  coordinates of the zone points. Reflective boundary conditions are applied to the  $r$  and  $z$  axes. In this problem compression results with respect to the cylindrical “ $r$ ” coordinate while net expansion develops with respect to the “ $z$ ” coordinate. The grid is shown in Fig. 7(a) at the final time of 0.8 (valid in any consistent set of units). It is very regular with large compression occurring near the origin. In this region where the analytic solution is valid (the region where the rarefaction wave that propagates inward from the outer boundary has not yet reached) the density should be flat with a value of 37.4. In Fig. 7(b) is shown the density plotted as a function of distance from the origin for the zones along all ten  $k$ -lines for two cases: the solid lines are for the standard case with limiters on and viscosity coefficients  $c_1$  and  $c_2$  set to unity; the dotted lines give this result for the same conditions except that the limiters are turned off. We see that inside a major radius of 0.2, the standard case with the limiters on gives results close to the correct value. With the limiters off the artificial viscosity turns on substantially giving answers that vary greatly along different  $k$ -lines and are very far from the true solution. Figure 7(c) shows the same set of results except that now the solid curves are the answer when the viscosity coefficients  $c_1$  and  $c_2$  are set to zero, and thus

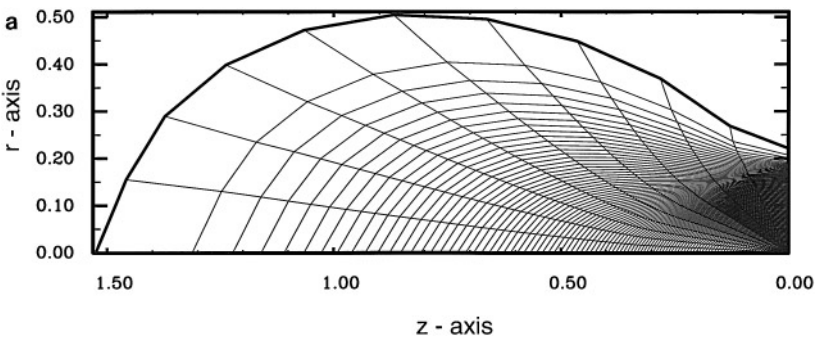


**FIG. 7.** (a) Adiabatic compression problem: grid at final time of 0.8. (b) Adiabatic compression problem: solid curves, density as a function of major radius along all  $k$ -lines for standard case at time 0.8; dotted curves, density as a function of major radius along all  $k$ -lines with all limiters off at time 0.8. (c) Adiabatic compression problem: solid curves, density as a function of major radius along all  $k$ -lines with viscosity off  $c_1 = c_2 = 0.0$  at time 0.8; dotted curves, density as a function of major radius along all  $k$ -lines with all limiters off at time 0.8.

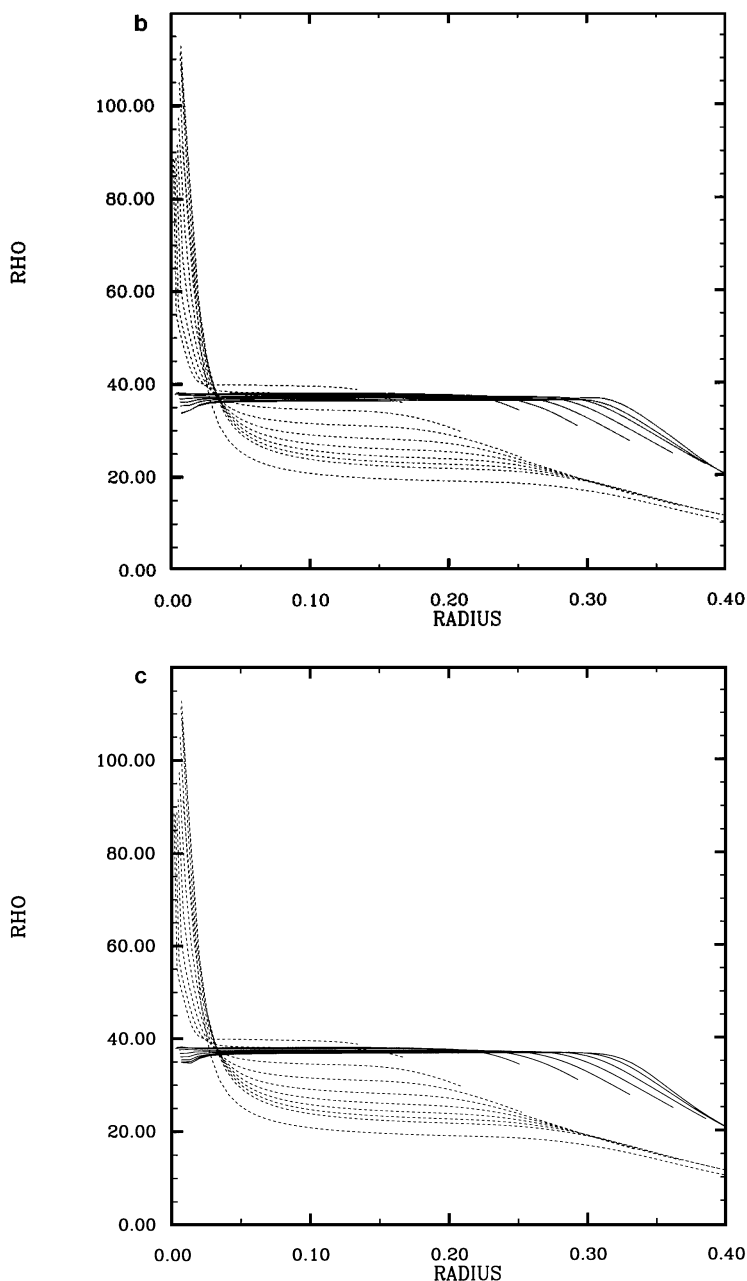
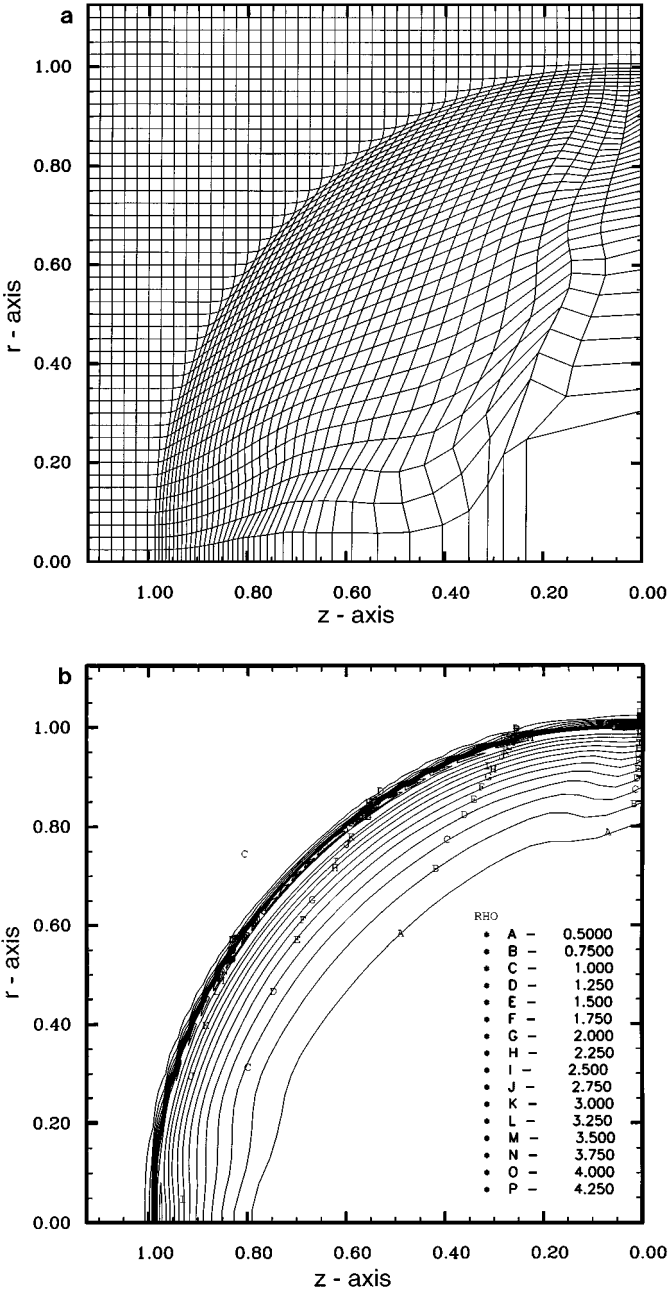


FIG. 7—Continued

corresponds exactly to the isentropic flow conditions of this problem. There is very little difference between this case and the standard case of Fig. 7(b) where these parameters were set to unity and the limiters were on. Thus the limiters have been very effective in detecting adiabatic motion and turning off the artificial viscosity.

Finally, we present results of the Sedov blast wave [26] in a cylindrical coordinate system as an example of a diverging shock wave, both with and without the artificial viscosity limiters. Our initial setup consists of a square grid with an edge of length 1.125 divided



**FIG. 8.** (a) Sedov blast wave: grid at time 1.0 for standard case. (b) Sedov blast wave: density contour plot at time 1.0 for standard case. (c) Sedov blast wave: grid at time 1.0 with all limiters off. (d) Sedov blast wave: density contour plot at time 1.0 with all limiters off.

into  $45 \times 45$  square zones. Two of the edges of the square correspond to the  $r$  and  $z$  axes where reflective boundary conditions are enforced. The initial density is unity and the initial velocity is zero. The specific internal energy is zero except in the first zone where it has a value of 5027.7. The analytic solution predicts that the shock should be at a major radius of unity at a time equal to unity with a peak density of four. In Fig. 8(a) the

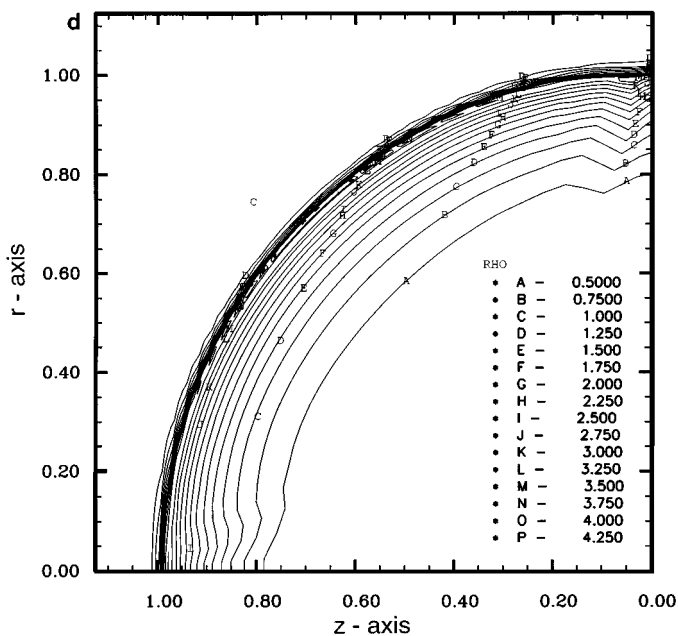
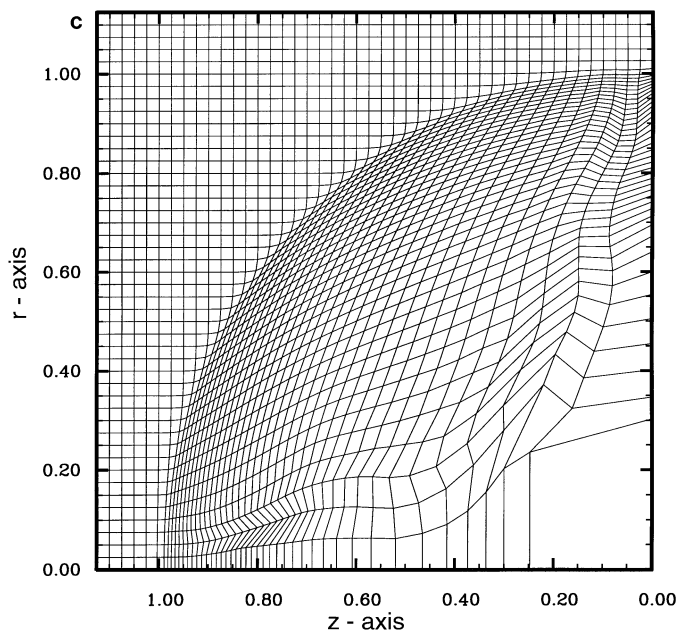


**FIG. 8—Continued**

grid is shown at this time for the standard case with the limiters turned on. Note that the shock wave has not quite reached 1.0 on the  $z$ -axis and is slightly beyond it with respect to the  $r$ -axis. This occurs because the initial energy source was not spherical, but was instead cylindrical, owing to the coordinate system. The grid is smooth as is the contour plot of the density shown in Fig. 8(b). In Fig. 8(c) the grid is shown at the final time for an identical run except that the artificial viscosity limiters have been turned off. The

grid shows some modest distortion along both the  $r$  and  $z$  axes. This can also be seen in the contour plot of the density given in Fig. 8(d). Therefore, this example shows that while the limiters do give an improved result in that the density contours are smoother, this improvement is not nearly as great for expanding divergent shock flow as it is for convergent flow.

### 5.1. *Inherent Difficulties*

The artificial viscosity method strictly applies to steady-state shock wave situations, where it potentially gives correct answers. However, if a shock wave intersects a rigid wall, encounters a sharp change in density as occurs at an interface between materials, or simply propagates across a grid whose initial spacing is variable, errors in the solution will occur. These errors are inherent in this method. They were first analyzed in one dimension by Cameron [27] who suggested various adjustments in the coefficients of the artificial viscosity and in the initial grid spacing to compensate for them. Margolin *et al.* [28] also analyzed these difficulties and proposed scaling the form of the gradient operator used to compute the force in order to correct them. However, all of these fixes were for one dimension and do not readily generalize to multi-dimensions. The error associated with nonuniform initial grid spacing in a single material is essentially a result of the fact that the artificial viscosity spreads a shock over a fixed number of cells giving a shock width that depends on grid spacing rather than on any physical scale [28]. The errors that occur at a boundary are of a different character. These errors are like the wall heating error seen in Noh's problem in Fig. 5. We give a further discussion of these since they have given rise to the idea that one should include in the equations an artificial heat flux that is directly linked to the artificial viscosity [24].

In the Noh problem the heating due to the artificial viscosity is too high near the origin and the density there is thus too low because the pressure adjusts to be nearly a constant in the shocked region. The difficulty in this case is that the artificial viscosity turns on sharply at the discontinuity in the velocity field that occurs initially at the origin. This is in contrast to a running shock wave where the viscosity turns on and off slowly, more like a half wavelength sine function, and less heating occurs in a given zone. Noh suggests the addition of an artificial heat flux into the internal energy equation to remedy spurious wall heating [24]. An artificial coefficient of thermal conductivity can be easily constructed based on the nonlinear part of the artificial viscosity. For  $q = \rho(\Delta \mathbf{v}_i)^2$ , and from simple dimensional considerations, the associated coefficient of thermal conductivity is  $\kappa = |\rho \Delta \mathbf{v}_i \cdot \Delta \mathbf{x}_i|$ . It is not at all clear from first principles that this term can be justified. However, an artificial heat flux is easy to implement. One just uses the same limiters and on/off criteria that were a part of the artificial viscosity to control and limit the  $\kappa$  just given. Then this coefficient is inserted into a diffusion term that is now part of the equation for specific internal energy. Because of the factor of  $\Delta \mathbf{x}_i$  in  $\kappa$ , this term obeys the same CFL stability condition as the explicit hydro scheme and thus causes no additional timestep limitations. Although the wall heating error seen in Fig. 5 can be substantially eliminated with this simple procedure and a large enough constant in front of  $\kappa$ , we find that for the same parameter settings this causes significant spreading of contact discontinuities on other test problems. This spreading is due mostly to numerical noise since  $\kappa \approx |\Delta \mathbf{v}_i|$  across a zone, which is zero for an idealized contact discontinuity. However, for this reason we have not found the heuristic concept of an artificial heat flux to be acceptable.

## 6. SUMMARY AND CONCLUSIONS

The issues of concern in the specification of a useful artificial viscosity for the simulation of shock wave problems in more than one dimension have been investigated. Artificial viscosity was first discussed in one dimension in order to detail the origins of this term, and also, to set the framework for the development given in the multi-dimensional case. In one dimension the difficulty in constructing an artificial viscosity is to ensure that it vanishes for uniform compression.

In the multi-dimensional case qualitatively different and more difficult issues are confronted. First, one can consider more than one centering for the artificial viscous term: in the zones like the pressure in a staggered grid formulation, or along the edges of a given zone. Next there is the issue of “dissipativity” that by definition every form of artificial viscosity must satisfy. A set of additional criteria that any reasonable artificial viscosity should obey was given. It was shown how these criteria could be satisfied with a properly formulated edge-centered artificial viscosity; this result constitutes the major achievement of this work.

Central to this formulation was the generalization to multi-dimensions of Christiansen’s idea [4] of using one-dimensional advection limiters to control the magnitude of the artificial viscosity along any given edge of a zone. This was effected in a simple and straightforward manner to obtain “intelligent” forms of artificial viscosity that are able to distinguish between adiabatic and shock compression. Although our entire discussion was given in two dimensions, all arguments are applicable to any number of dimensions and for grids that are either logically rectangular or unstructured. The viscous forces are simply computed with respect to a given edge of a zone on the appropriately defined median mesh that always yields the compression condition, and with limiter functions computed with respect to appropriately defined left and right line segments.

Although numerical results using the edge-centered artificial viscosity specified herein have been given as part of a larger piece of work [2, 19, 22], numerical examples were presented to show its sensitivities to coefficients and limiters for various flow regimes. These results, in conjunction with the aforementioned larger set, are meant to show that the artificial viscosity method need not be considered spurious or arbitrary in its implementation or effectiveness. This suggests that this method is a viable alternative to Riemann solvers of various types that have been utilized for the solution of high speed flow calculations. The artificial viscosity method affords great relative simplicity in multi-dimensions because there is no need to spatially split the equations with respect to each dimension, and because the complexity of the algorithm does not fundamentally increase when increasingly complicated physical effects are included.

### APPENDIX: SUMMARY OF EDGE VISCOSITY

In order to facilitate coding, the artificial viscous force developed in Section 4 is written out in complete form with all relevant formulas collected together. This is done for the two points  $b$  and  $c$  of Fig. 2 where we have assumed a staggered spatial placement of variables with coordinates and velocity defined at points and all other variables defined inside zones. The viscous force that acts between these two points we label as  $\mathbf{f}_i$ , where  $i = 1$ . (We retain the  $i$  subscript to indicate that this could be any other edge.) This force is due to the shaded region with median mesh vector  $\mathbf{S}_1$  defined as the normal to, and with magnitude of, the line joining the zone center to the edge midpoint. The velocity difference between these

points is defined as  $\Delta \mathbf{v}_{i=1} \equiv \mathbf{v}_b - \mathbf{v}_c$ , and the unit vector in the direction of this difference is  $\widehat{\Delta \mathbf{v}}_{i=1}$ . Given these definitions and using Eq. (20) in conjunction with the Kuropatenko form of the basic scalar artificial viscosity, Eq. (8), this force is written in full as

$$\mathbf{f}_{i=1} = \rho_i \left\{ c_2 \frac{(\gamma + 1)}{4} |\Delta \mathbf{v}_i| + \sqrt{c_2^2 \left( \frac{\gamma + 1}{4} \right)^2 (\Delta \mathbf{v}_i)^2 + c_1^2 c_{s,i}^2} \right\} \\ \times (1 - \psi_i) (\Delta \mathbf{v}_i \cdot \mathbf{S}_1) \widehat{\Delta \mathbf{v}}_i \quad \text{if } (\Delta \mathbf{v}_i \cdot \mathbf{S}_1) \leq 0, \quad (21)$$

$$\mathbf{f}_{i=1} = 0 \quad \text{if } (\Delta \mathbf{v}_i \cdot \mathbf{S}_1) > 0, \quad (22)$$

where we next define the remaining quantities in this expression. Then we comment on how this force is used in the equations for the evolution of momentum and internal energy.

The coefficients  $c_1$  and  $c_2$  that multiply the strengths of the linear and nonlinear viscosity terms, respectively, are always set as  $c_1 = c_2 = 1$ . The ratio of specific heats  $\gamma$  of a substance lies in the range  $1 \leq \gamma \leq 3$ . The density  $\rho_{i=1}$  and the speed of sound  $c_{s,i=1}$  are given by

$$\rho_{i=1} = \frac{2\rho_b\rho_c}{(\rho_b + \rho_c)}, \quad (23)$$

$$c_{s,i=1} = \min(c_{s,b}; c_{s,c}), \quad (24)$$

where the density and the sound speed at the points  $b$  and  $c$  are defined as area weighted averages of their values with respect to the zones surrounding these points for the case where all of these zones are composed of the same material. If differing materials border either of these points then Eqs. (23), (24) are ignored and we set  $\rho_{i=1}$  and  $c_{s,i=1}$  to the values of these quantities present in the zone that contains the vector  $\mathbf{S}_1$ . Next the limiter function  $\psi_{i=1}$  is computed as

$$\psi_i = \max[0., \min(.5(r_{l,i} + r_{r,i}), 2r_{l,i}, 2r_{r,i}, 1.)]. \quad (25)$$

The arguments of this function are given by Eq. (18), repeated here as

$$r_{l,i} = \frac{\Delta \mathbf{v}_{i+1} \cdot \widehat{\Delta \mathbf{v}}_i}{\Delta \mathbf{x}_{i+1} \cdot \widehat{\Delta \mathbf{x}}_i} \bigg/ \frac{|\Delta \mathbf{v}_i|}{|\Delta \mathbf{x}_i|}, \quad r_{r,i} = \frac{\Delta \mathbf{v}_{i-1} \cdot \widehat{\Delta \mathbf{v}}_i}{\Delta \mathbf{x}_{i-1} \cdot \widehat{\Delta \mathbf{x}}_i} \bigg/ \frac{|\Delta \mathbf{v}_i|}{|\Delta \mathbf{x}_i|}. \quad (26)$$

The various factors, in addition to  $\Delta \mathbf{v}_i$  that has already been given, that appear in Eq. (26) are defined with reference to Fig. 2 as  $\Delta \mathbf{x}_i \equiv \mathbf{x}_b - \mathbf{x}_c$ ,  $\Delta \mathbf{x}_{i+1} \equiv \mathbf{x}_c - \mathbf{x}_d$ ,  $\Delta \mathbf{x}_{i-1} \equiv \mathbf{x}_a - \mathbf{x}_b$ ,  $\Delta \mathbf{v}_{i+1} \equiv \mathbf{v}_c - \mathbf{v}_d$ ,  $\Delta \mathbf{v}_{i-1} \equiv \mathbf{v}_a - \mathbf{v}_b$ , where  $\mathbf{x}_*$  or  $\mathbf{v}_*$  is the coordinate vector or velocity, respectively, of any point  $*$ . The unit vector directions associated with these differences are indicated by the carat superscript over the entire quantity. If the effective edge Courant condition  $(|\Delta \mathbf{v}_i|/|\Delta \mathbf{x}_i|)\Delta t$  is less than the roundoff error level ( $\sim 10^{-14}$ ), then  $r_{l,i}$  and  $r_{r,i}$  are set to unity. Recall that a boundary specification is needed for any  $r_{l,i}$  or  $r_{r,i}$  that falls outside of the given problem domain. In the case of reflective boundary conditions data are known that allows this missing factor to be directly computed; for other boundary conditions we either set it to unity or to the opposite known function,  $r_{l,i}$  or  $r_{r,i}$ . Also, if the underlying grid does not have a logical structure then the definitions of what is left and right with respect to a given edge must be defined as mentioned in Subsection 4.3 so that one knows what line segments to use in computing  $r_{l,i}$  and  $r_{r,i}$ .

Next the force  $\mathbf{f}_{i=1}$  must be assigned to the points  $b$  and  $c$  in the discrete momentum equation with proper signs. Each point obtains two contributions from each of its adjacent zones, or, eight viscous force contributions to each point of a quadrilateral grid. Given our sign convention in Fig. 2 that  $\Delta \mathbf{v}_{i=1} \cdot \mathbf{S}_1 \leq 0$  corresponds to compression of the edge “ $b - c$ ” with respect to the zone containing  $\mathbf{S}_1$ , we have from Eq. (21) that  $\mathbf{f}_{i=1} \sim -\widehat{\Delta \mathbf{v}_{i=1}}$ . It now follows that  $\mathbf{f}_{i=1}$  must be assigned to point  $b$  with a  $+$  sign and to point  $c$  with a  $-$  sign in order to resist  $\Delta \mathbf{v}_i$ . (To see this set  $\mathbf{v}_b = 0$ , and let  $\mathbf{v}_c$  lie parallel to  $\mathbf{S}_1$ .) The same logic is used to obtain the correct signs of these forces with respect to all edges of all zones.

Last, recall that in general for a staggered spatial grid, the rate of work done by any force  $\mathbf{f}_i$  with respect to the zone in which it is computed due to its action on a given point  $*$  is  $-\mathbf{f}_i \cdot \mathbf{v}_*$ . Thus the rate of work done by the force  $\mathbf{f}_{i=1}$  with respect to the zone in which it is defined is  $-\mathbf{f}_{i=1} \cdot (\mathbf{v}_b - \mathbf{v}_c) = -\mathbf{f}_{i=1} \cdot \Delta \mathbf{v}_i \sim \widehat{\Delta \mathbf{v}_i} \cdot \Delta \mathbf{v}_i$ , and is seen to be positive-definite as required. This is one term of the internal energy equation, previously given as Eq. (15). This equation must be used to compute the work done by these forces with respect to each zone.

The complete edge-centered artificial viscosity is implemented by coding the above expressions along every edge of every zone of a grid that can be composed of any kind of zone elements. We find it convenient to first compute all limiter functions,  $\psi_i$ , before computing the viscous forces with respect to the entire grid on a zone by zone basis.

## ACKNOWLEDGMENTS

We thank D. Burton, M. Clover, C. Cranfill, L. Margolin, and W. Rider for many useful and stimulating discussions of the artificial viscosity concept.

## REFERENCES

1. J. VonNeumann and R. D. Richtmyer, A method for the numerical calculation of hydrodynamic shocks, *J. Appl. Phys.* **21**, 232 (1950).
2. E. J. Caramana, D. E. Burton, M. J. Shashkov, and P. P. Whalen, The development of compatible hydrodynamics algorithms utilizing conservation of total energy, *J. Comput. Phys.*, in press.
3. W. D. Schulz, Two-dimensional Lagrangian hydrodynamic difference schemes, *Methods Comput. Phys.* **3**, 1 (1964).
4. R. B. Christiansen, *Godunov Methods on a Staggered Mesh—An Improved Artificial Viscosity*, Lawrence Livermore National Laboratory Report, UCRL-JC-105269, 1991.
5. D. J. Benson and S. Schoenfeld, A total variation diminishing shock viscosity, *Comput. Mech.* **11**, 107 (1993).
6. R. Landshoff, *A Numerical Method for Treating Fluid Flow in the Presence of Shocks*, Los Alamos National Laboratory Report, LA-1930, 1955.
7. M. L. Wilkins, Use of artificial viscosity in multidimensional shock wave problems, *J. Comput. Phys.* **36**, 281 (1980).
8. A. P. Favorskii, L. V. Moiseenko, V. F. Tishkin, and N. N. Tyurina, The introduction of artificial dissipators into finite-difference schemes of hydrodynamics, preprint, No. 18, M. V. Keldysh Institute of Applied Mathematics, Moscow, Russia, 1982.
9. N. V. Mikhailova, V. F. Tishkin, N. N. Turina, A. P. Favorskii, and M. Yu. Shashkov, Numerical modelling of two-dimensional gas-dynamic flows on a variable structure mesh, *USSR Comput. Math. and Math. Phys.* **26**, 74 (1986).
10. R. D. Richtmyer and K. W. Morton, *Difference Methods for Initial-Value Problems* (Interscience, New York, 1967), p. 313.

11. B. van Leer, Towards the ultimate conservative difference scheme 5: A second order sequel to Godunov's method, *J. Comput. Phys.* **32**, 101 (1979).
12. J. K. Dukowicz, A general, non-iterative Reimann solver for Godunov's method, *J. Comput. Phys.* **61**, 119 (1985).
13. V. F. Kuropatenko, in *Difference Methods for Solutions of Problems of Mathematical Physics, 1*, edited by N. N. Janenko (Amer. Math. Soc., Providence, 1967), p. 116.
14. D. Mihalas and B. Mihalas, *Foundations of Radiation Hydrodynamics* (Oxford Univ. Press, London, 1984), p. 283.
15. L. D. Landau and E. M. Lifshitz, Course of theoretical physics, in *Fluid Mechanics* (Pergamon, Elmsford, NY, 1982), Vol. 6, p. 48.
16. A. Harten, High resolution schemes for hyperbolic conservation laws, *J. Comput. Phys.* **49**, 357 (1983).
17. D. E. Burton, Exact conservation of energy and momentum in staggered-grid hydrodynamics with arbitrary connectivity, in *Advances in the Free Lagrange Method* (Springer-Verlag, New York, 1990).
18. W. D. Schulz, unpublished notes, 1979.
19. E. J. Caramana and M. J. Shashkov, Elimination of artificial grid distortion and hourglass-type motions by means of Lagrangian subzonal masses and pressures, *J. Comput. Phys.* **142**, 521 (1998).
20. D. E. Burton, *Multidimensional Discretization of Conservation Laws for Unstructured Polyhedral Grids*, Lawrence Livermore National Laboratory Report, UCRL-JC-118306, 1994.
21. D. E. Burton, private communication.
22. E. J. Caramana and P. P. Whalen, Numerical preservation of symmetry properties of continuum problems, *J. Comput. Phys.* **141**, 174 (1998).
23. L. G. Margolin, *A Centered Artificial Viscosity for Cells with Large Aspect Ratio*, Lawrence Livermore National Laboratory Report, UCRL-53882, 1988.
24. W. F. Noh, Errors for calculations of strong shocks using an artificial viscosity and an artificial heat flux, *J. Comput. Phys.* **72**, 78 (1987).
25. S. V. Coggeshall and J. Meyer-ter-Vehn, Group invariant solutions and optimal systems for multidimensional hydrodynamics, *J. Math. Phys.* **33**, 3585 (1992).
26. L. I. Sedov, *Similarity and Dimensional Methods in Mechanics* (Academic Press, New York, 1959).
27. I. G. Cameron, An analysis of the errors caused by using artificial viscosity terms to represent steady-state flow, *J. Comput. Phys.* **1**, 1 (1966).
28. L. G. Margolin, H. M. Ruppel, and R. B. Demuth, *Gradient Scaling for Nonuniform Meshes*, Los Alamos National Laboratory Report, presented to Fourth International Conference on Numerical Methods in Laminar and Turbulent Flow, 1985.